Hindawi
Geofluids
Volume 2022, Article ID 1601398, 14 pages
https://doi.org/10.1155/2022/1601398

Research Article

Experimental Study on Frost Heave Behavior of Steel Fiber Improved Soil

Rongjian Shi,[1] **Feng Huang**,[2] **Fengtian Yue**,[2] **Zequn Hong**,[2] **and Yichen Li**[3]

[1]*State Key Laboratory for Geomechanics and Deep Underground Engineering, School of Mechanics and Civil Engineering, China University of Mining and Technology, Xuzhou 221116, China*
[2]*School of Mechanics and Civil Engineering, China University of Mining and Technology, Xuzhou 221116, China*
[3]*Xuzhou Construction Engineering Testing Center Co. LTD., Xuzhou 221003, China*

Correspondence should be addressed to Rongjian Shi; rjshi@cumt.edu.cn

Received 28 July 2022; Accepted 9 September 2022; Published 24 September 2022

Academic Editor: Yu Wang

The incorporation of steel fibers into the natural soil is generally considered to be a novel and effective way to reduce the amount of frost heave induced by an artificial freezing process in underground engineering. In order to analyze the frost heave behavior of the steel fiber improved soil, a one-dimensional frost heave test under the open recharge system was conducted in this paper, focusing on the influence of steel fiber content, size, and soil properties. The results show that small amounts of steel fibers in the soil will not significantly affect the freezing process and temperature distribution, while the water-conducting properties of the steel fibers and the effect of limiting the ice lens growth can reduce the frost heave rate of the samples incorporated with 0.5% steel fibers by 26.93%. At the same time, the reduction effect of the frost heave rate increases linearly with the increase of steel fiber content and length but weakens with the increase of steel fiber diameter. In terms of soil property influence, the frost heave rate of the clay samples was reduced by 14.31% compared to the silt samples, while the water migration was reduced by 11.99%. In addition, the cementation of the steel fibers with the soil will also inhibit the growth of the ice lens and reduce the external water migration, thus significantly lowering the frost heave rate. The results can provide a reference for the research of the frost deformation of similar modified soils.

1. Introduction

Frost heave deformation is an inevitable hazard in the artificial freezing process, which often causes serious damage to surrounding buildings or underground pipelines and even threatens the safety of the structure [1, 2]. Effective control of frost heave has always been the key to the successful application of the artificial ground freezing method. Frost heave is a complex process involving multiphysics coupling, which is significantly affected by freezing construction parameters [3]. It has been shown that factors affecting the water-holding capacity of soil particles, such as soil properties, fine-grained soil content, and dry density, all have a significant effect on frost heave [4, 5]. Construction factors such as temperature gradient and freezing speed during the freezing process will change the water migration and thus affect the amount of frost heave [6]. In addition, environmental factors such as soil compaction energy [7], binding force around frozen soil [8], and freezing mode will also have a certain impact on frost heave [9].

Based on the influencing factors and generation mechanism of frost heave, scholars have also proposed a series of methods to control this deformation. Shen et al. proposed to set stress release holes in the soil to reduce the frost force [10] and analyzed the differences with conventional freezing in terms of temperature distribution, frost heave rate, and water migration. Zhou Jet al. studied the law of frost heave under different construction modes through a one-dimensional freezing test [11, 12] and found that the amount of frost heave under an intermittent freezing mode is only about 40% of that under continuous freezing. Zhou and Zhou further revealed the mechanism of the intermittent freezing mode to reduce frost heave in terms of temperature gradient and water mobility [13]. By studying the effect of

different loading paths on the frost heave of silty clay, Huang et al. found that the additional force can inhibit the migration of water in the soil [14], thereby reducing the amount of frost heave. The relatively small extent and volume of frozen soil formed by municipal artificial freezing make it possible to control the effects of frost heave by improving the ground soil. An experimental study on lime incorporated strata found that the porosity and hydraulic conductivity of the ground soil decreased with the lime content, resulting in a significant reduction in the frost heave rate [15]. Tan and Hu found that the incorporation of cement in the stratum would consume the water in the soil and reduce the permeability coefficient [16, 17], thus hindering water migration and reducing the partitioning effect of ice, and now, the cement modified method has been successfully applied in engineering [18]. In addition, Li et al. also proposed a method to use soil bags to prevent the migration of capillary water and film water in cold regions to suppress frost heave [19]. Incorporating a viscous gel formed by incorporating nanosilica into the silty clay to block the migration of water in the soil was also proved to be effective to reduce the frost heave rate [20]. But the engineering applications show that the generated chemical reactions when materials such as cement and silica are incorporated into the soil layer can cause irreversible changes in the properties of the soil, thus limiting the scope of application of soil improvement methods. In terms of reinforced soil, Chen et al. found that the frost heave amount can be reduced by about 27% when the soil is improved with polyester fibers [21]. Liu et al. studied the frost heave characteristics of the soil mixed with rubber particles [22], asphalt, and polypropylene fibers and found that the increase in the content of rubber particles has a negative effect on the inhibition of frost heave, while the smaller elastic modulus of the mixture and the capillary rupture effect are both positive to improve the suppressing of frost heave deformation.

Different from the direct mixing of organic fibers in the subgrade soil in cold regions, the fibers mixed into the stratum by means of rotary spray reinforcement generally need to use steel fibers with high strength and rigidity in the reinforcement improvement construction of municipal engineering. Studies have found that incorporating a small amount of steel fibers can significantly change the nature of soil and improve its mechanical properties [23, 24]. The parameter changes in the thermophysical and mechanical properties can affect the water migration and the growth process of the ice leaching, which affects the defensive deformation during freezing [25, 26]. These existing researches qualitatively show that steel fiber plays a positive role in reducing the environmental disturbance of frost heave when it is applied to the artificial ground freezing method, but there is still a lack of mechanism and quantitative analysis of steel fiber improved soil to inhibit frost heaving. Through the one-dimensional frost heave test in the open recharge system, this paper analyzes the influence law of the fiber length, diameter, and content on the frost heave behavior of the modified soil. The research results can provide a theoretical reference for the method of controlling frost heave hazards using steel fiber improved soil.

Table 1: Basic properties of experimental soil.

Soil samples	Plastic limit (%)	Liquid limit (%)	Dry density ($g \cdot cm^{-3}$)
Silty clay	16.8	32.8	1.35
Silt	18.1	26.9	1.38

Table 2: Dimensional and thermophysical parameters of steel fiber in the test.

Basic parameters	Value ranges	Density ($g \cdot cm^{-3}$)	Thermal conductivity ($W \cdot (m \cdot k)^{-1}$)
Length l (mm)	8, 10, 13	7.8	16.28
Diameter d (mm)	0.12, 0.2, 0.3		
Mass content c (%)	0.25, 0.5, 0.75		

2. Test Protocol and Process

2.1. Test Scheme and Preparation of the Modified Soil. Two soil layers, silty clay and silt, which are highly sensitive to frost heave in Shanghai, were selected for this test. The chosen steel fibers were conventional straight copper-coated steel fibers. The parameters of soil layers and steel fibers are shown in Tables 1 and 2. Steel fibers were added to the two soil layers according to the parameters in Table 2, and orthogonal combination tests with different parameters were carried out to analyze the influence of fiber size on the frost heave process.

In order to improve the uniformity of the distribution of steel fibers in the prepared samples, the undisturbed soil was first dried and pulverized, then mixed with water, and the soil samples were weighed and bagged according to the design density. According to the different quality and dosage of steel fibers, they are mixed with dry soil, respectively, to ensure that the steel fibers are evenly dispersed in the soil. Next, spray the required amount of water to saturate the soil sample on the surface of the soil sample and then stir it evenly. Repeat several times until the water and the soil sample are fully mixed and then put it in a sealed bag and stand for 24 hours to ensure that the water is fully diffused and evenly distributed in the soil sample.

2.2. Test Equipment and Monitoring Program. The frost heave test process was carried out in accordance with the "Standards for Geotechnical Test Methods" (No. GB/T50123-2019) in China. The test instrument used is a low-temperature frost heave test box of XT5412-MTC192, which consists of a standard sample cylinder, a heat-conducting plate, a test environment chamber, a cold bath, a Mariotte bottle, and a temperature and displacement sensor; the schematic diagram of the test system is shown in Figure 1. In this system, the inner diameter of the standard sample cylinder is 100 mm, the height is 90 mm, and the wall thickness is 10 mm. The two heat-conducting plates at the bottom and the top of the sample are independently connected to the

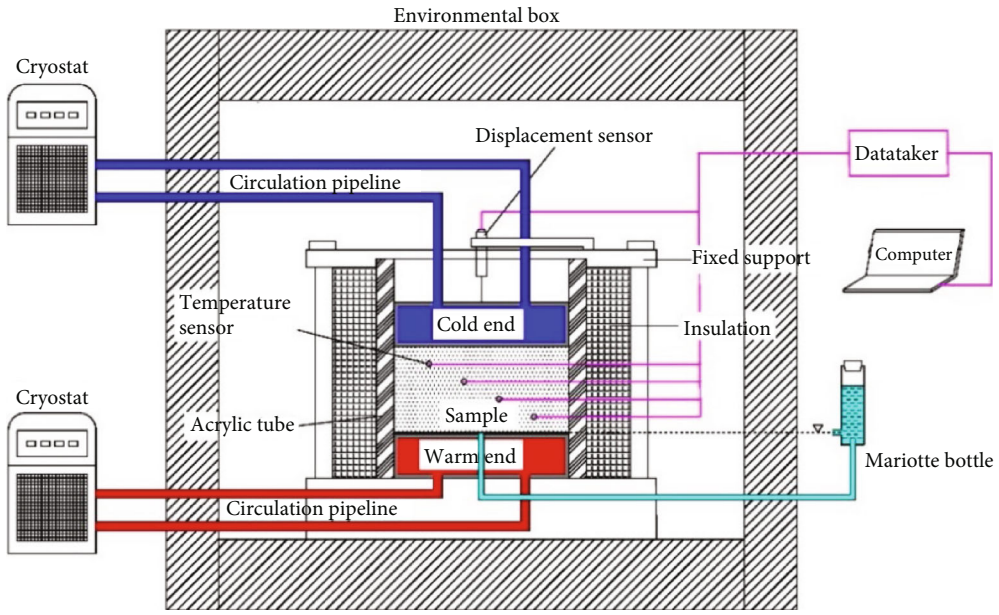

Figure 1: Schematic diagram of the test system.

two cooling baths. The freezing process of the sample is controlled by adjusting the temperature of the cooling bath. The environmental box is used to control the stability of the ambient temperature during the test. The inner diameter of the Mariotte bottle is 30 mm, and the range is 200 ml, which ensures that the lateral vent is flush with the water supply surface and realizes pressure-free water supply during the freezing process.

Divide the prepared steel fiber modified soil into 5 equal parts, put it into the sample cylinder, and compact them to 50 mm. After the samples meet the requirements, vacuum saturation work is carried out. During the freezing process, the cold end of the top plate is kept at -10°C, and the warm end of the bottom plate is kept at 2°C which is the same as the temperature of the environmental box. Besides, the bottom of the sample is filled with water without pressure using a Mariotte water bottle. The debugged sample during the test is shown in Figure 2. In the test system, four temperature measurement points are arranged in a spiral shape from a position 10 mm from the bottom of the sample; the horizontal and vertical distances between adjacent temperature measurement points are 20 mm and 10 mm. In addition, a displacement sensor is installed above the cold end at the top of the soil sample to test the vertical heave deformation. Test data such as temperature, displacement, and water supply are monitored in real time through the DataTaterG85 data collector. The layout of the measuring points is shown in Figure 3.

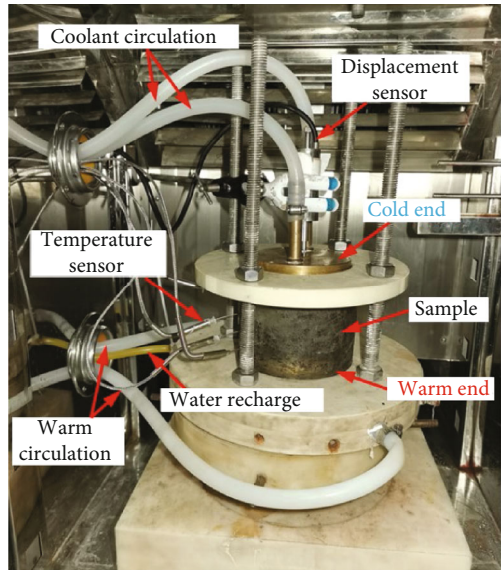

Figure 2: Schematic diagram of the test system.

3. Test Results

3.1. Temperature Variation. Control the steel fiber length l and diameter d as fixed values, which are 13 mm and 0.12 mm, respectively. When the steel fiber content c is 0 and 0.5%, the temperature change of the silt sample is shown in Figure 4.

It can be seen from Figure 4 that the temperature changes of the two samples during the freezing process are generally the same, and they have roughly experienced three stages of rapid cooling, slow cooling, and gradual stabilization. Directly affected by the top cold plate, the temperature of the measure point C4 at a distance of 10 mm from the top plate dropped the fastest and entered a negative temperature state after freezing for 10 minutes. After 120 minutes of freezing, the temperature change trend of each measuring point gradually slowed down and entered a slow cooling stage. After 250 minutes, the overall temperature of the

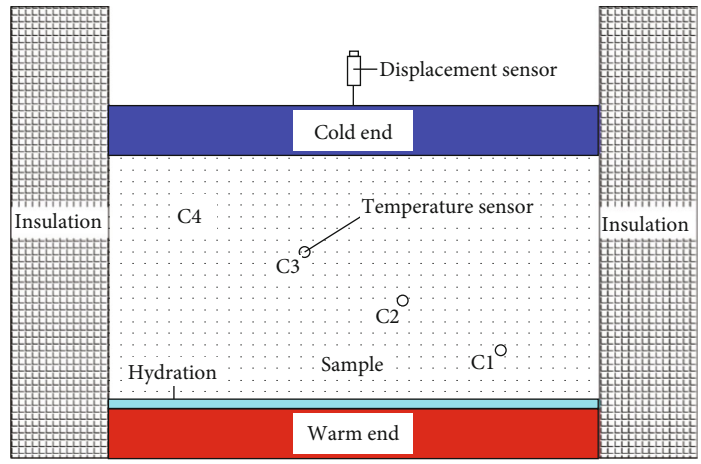

Figure 3: Layout of temperature and displacement measuring points.

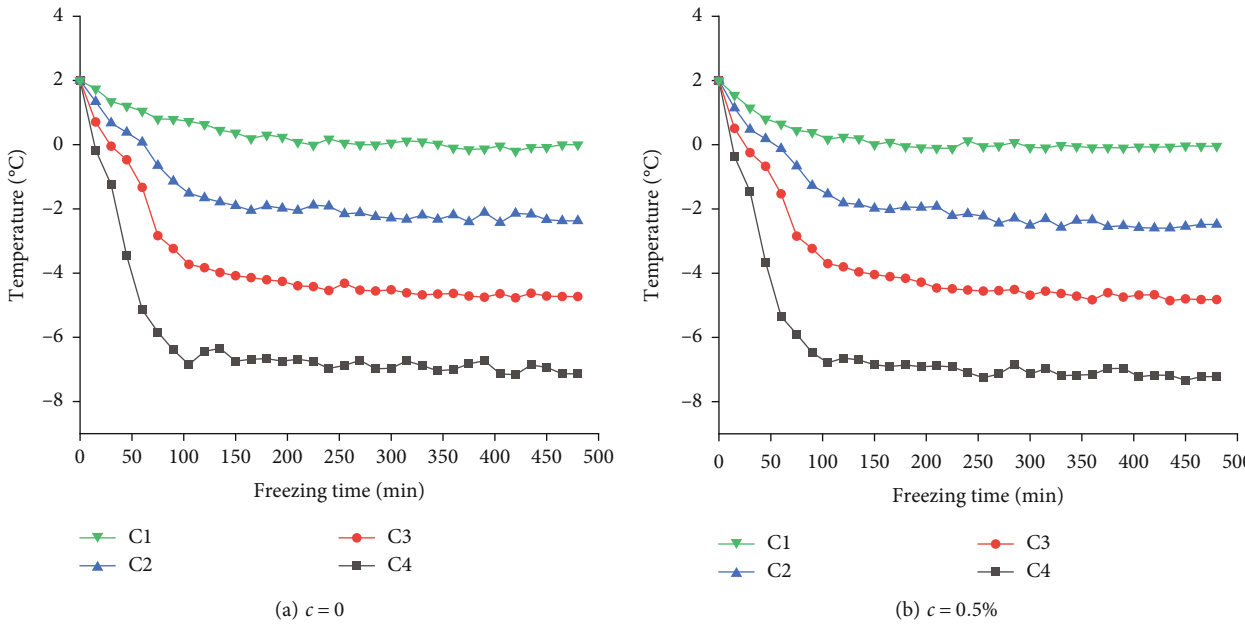

Figure 4: Curves of temperature change in the sample.

sample entered a stable stage, and the difference between each measurement point remained almost constant.

At the same time, by comparing Figures 4(a) and 4(b), it can be seen that no matter whether steel fibers are added or not, the time for the temperature of the measuring points at different heights to decrease to the negative temperature is basically the same, indicating that the advancing speed of the freezing front in the sample is not different. It is important to indicate that the freezing front in this paper refers to the position where the specimen temperature is equal to the freezing temperature, gradually moving from the top to the bottom as the freezing process proceeds. It can be determined in the test by interpolating the temperature monitoring points at different heights. In the temperature stabilization stage, the temperature and temperature difference of the measuring points are almost the same, which proves that the incorporation of a small amount of steel fibers into the sample will not significantly affect the freezing process of the sample.

3.2. Frost Heave Deformation Characteristics. Figure 5 shows the frost heave rate curves of silt samples under the condition of different steel fiber content c (the length and diameter are set to fixed values, $l = 8$ mm, $d = 0.12$ m). It can be found that after the start of freezing, the thermal expansion and contraction effect caused by the rapid cooling of the top soil causes the volume of the sample to shrink, resulting in a little settlement of the top cold plate, and the frost heave rate of the sample has a negative value, but the change is not large. In the rapid cooling stage within the first 120 minutes, the frost heave deformation grows slowly. The reason is that the rapid expansion of frozen soil in this stage shortens the water migration time, resulting in less water supplementation from the outside of the sample, and correspondingly,

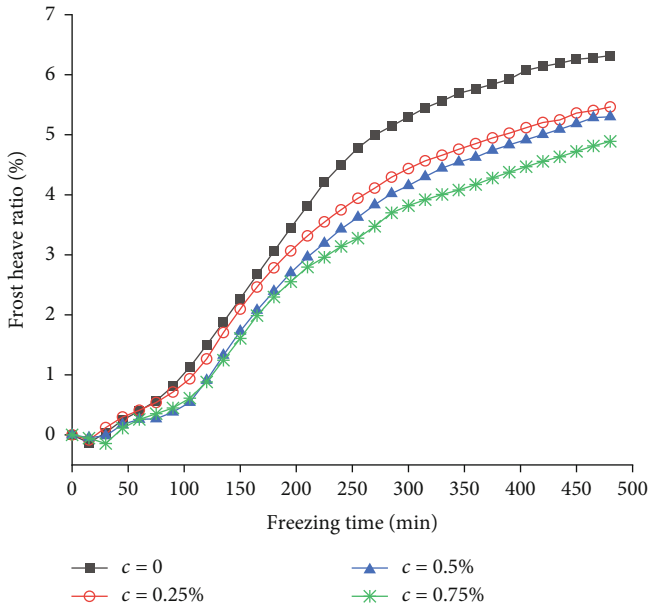

Figure 5: Frost heave rate curves with different steel fiber contents.

the amount of the generated segregated frost heave is also small. During the slow cooling stage from 120 min to 250 min, most of the temperatures dropped below 0°C; the decrease of the freezing front moving speed in the sample increases the time of water migration. A large amount of water supply makes the frost heave rate of the sample increase obviously, and the frost heave amount in this stage accounts for about 80% of the whole test stage. After 250 min of freezing, the temperature of the sample hardly changed, and the water recharge from outside was limited to the unfrozen area at the bottom of the sample. The smaller temperature gradient reduces the water migration speed, and the increase of overall deformation gradually slowed down, entering a stable stage.

Comparing the deformation curves of different steel fiber contents, it can be found that the evolution trend of the frost heave rate is generally consistent. In the rapid cooling stage, the overall frost heave rate of the samples before and after adding steel fibers was less than 1%. In the slow cooling stage after 120 min, the tensile strength was generated due to the cementation between the frozen soil and the steel fibers, thus inhibiting the frost heave deformation of the specimen. Therefore, the frost heave deformation of the samples mixed with steel fibers is smaller than that without steel fibers, and with the increase of the amount of steel fibers, the effect of inhibiting frost heave is more obvious, especially after 200 min. In the stable stage after 250 min, the cementation between the frozen soil and the steel fibers continued to strengthen, which limited the volume growth of the ice lens in the frozen soil and further increased the difference in the amount of frost heave deformation with different steel fibers. The frost heave rates of the samples with steel fiber content of 0.25%, 0.5%, and 0.75% were 5.46%, 5.29%, and 4.89%, respectively. Compared with 6.35% of the sample without steel fibers, the frost heave rate was reduced by 13.94%, 16.52%, and 22.98%. The test results show that the frost heave deformation can be effectively inhibited by adding a small amount of steel fibers to the sample.

3.3. Variation of Water Supplement. Under the condition of different steel fiber content c ($l = 8$ mm, $d = 0.12$ mm), the change curve of the cumulative amount of water supplement is shown in Figure 6.

It can be seen that in the early freezing stage, the curve is flat and the amount of water added is small. This is because the moving speed of the freezing front is fast in the first 90 minutes, and the redistribution of the initial water content can meet the needs of water migration at the position of the freezing front. As the freezing continues, when the freezing front advances to 20 mm from the bottom of the sample, the decrease in the advancing speed of the freezing front leads to a significant increase in the external water supply, and an ice lens is formed in the sample, resulting in a rapid increase in the frost heave rate. After freezing for 250 minutes, the freezing front developed to the bottom, which reduced the overall temperature gradient of the sample. Existing studies have shown that a small temperature gradient will reduce the water migration [27, 28], so that the external water supplementation will gradually decrease and reach a stable stage.

Comparing the cumulative water replenishment of samples with different steel fiber contents, it can be found that with the increase of steel fiber content, the strength of the formation of frozen soil will be improved, which will inhibit the growth of ice lens in the sample, thereby reducing the external water replenishment. At the end of freezing, the accumulative water supplement with steel fiber content of 0, 0.25, 0.5, and 0.75% was 17.2, 15.8, 14.4, and 13.9 ml, respectively. Combined with Figures 5 and 6, the time when the frost heave deformation is significantly different is about 100 min earlier than the time when the water supplement amount is different, which indicated that the addition of steel fibers into the sample would also affect the deformation process inside the sample when the water supplement amount was not much different. Therefore, steel fibers will not only affect the water migration during the freezing process but also affect the deformation process inside the soil, thereby affecting the effect of frost heave on the surrounding environment.

Furthermore, according to the second frost heave theory, the water migration path on the freezing front mainly occurs in the film water on the surface of soil particles, and the size of the soil is a key factor affecting the film water migration effect. Since the diameter of the incorporated steel fibers is much larger than the particle size of the silt, the water migration path is mainly around the silt particles during the freezing process. The incorporation of steel fibers will not increase the amount of water migration but will increase the water-conducting channels around the steel fibers, which will increase the water displacement of the samples during the frost heave compression process. Therefore, the amount of water replenishment at this stage will be slightly smaller than that of the samples without steel fibers.

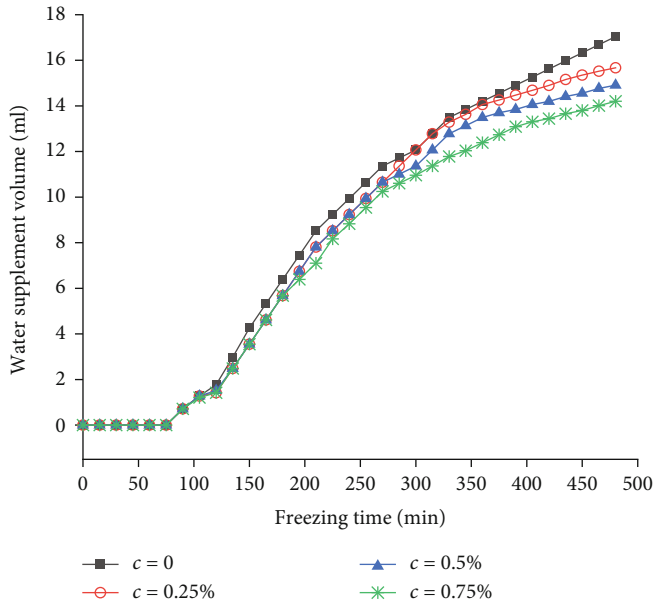

Figure 6: Water supplement variation of samples with different steel fiber contents.

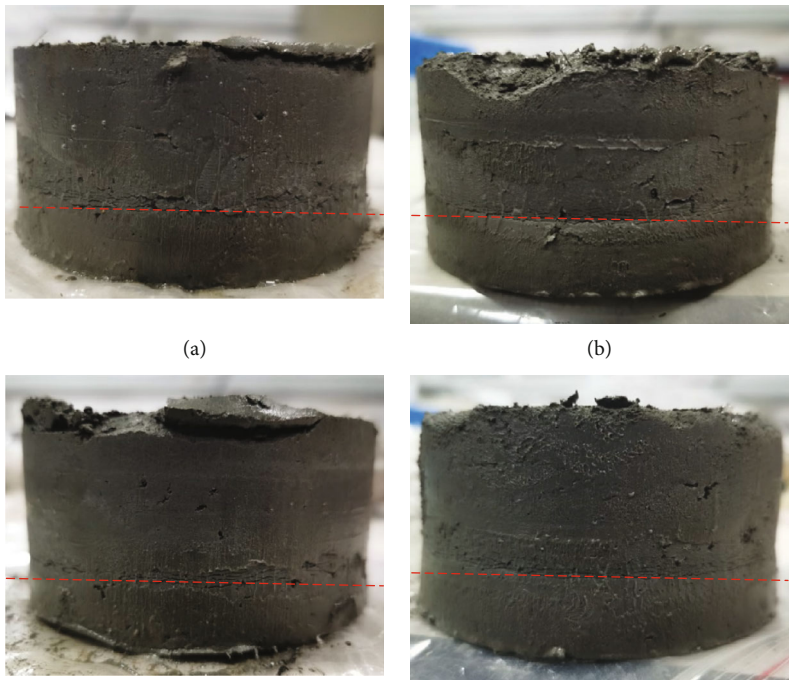

Figure 7: Frozen soil samples at the end of freezing: (a) $c = 0$; (b) $c = 0.25\%$; (c) $c = 0.5\%$; (d) $c = 0.75\%$.

3.4. Distribution of Moisture Content in the Sample. After the test, the samples with different steel fiber contents are shown in Figure 7, and the moisture content is measured by 10 mm slices along the height direction to analyze the distribution characteristics. The distribution curve of moisture content inside the sample is shown in Figure 8.

The freezing of water in the soil will fill the gaps between the particles and block the passage of water migration, so the water migration will only appear in the unfrozen area of the sample, and the frozen part will not continue to replenish water from the outside. It can be seen from Figure 7 that after freezing from the top of the sample, there is no obvious ice condensation layer in the upper part, but an ice lens is formed in the lower part of the sample. The positions of the ice lenses formed under the conditions of different steel fiber contents are basically the same, which are manifested as obvious wrinkles in the lower part of the sample. This is because the temperature gradient-induced moisture

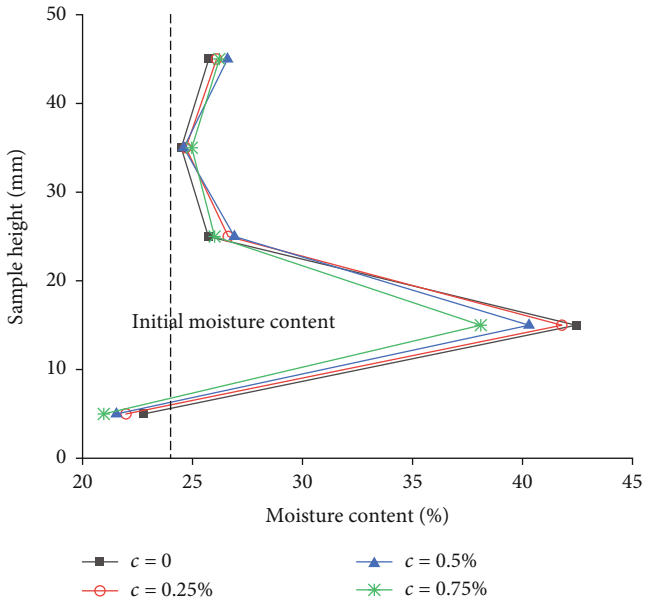

Figure 8: Moisture distribution curves with different steel fiber contents.

migration increases significantly and the location of the ice lens formation is not much different. From the appearance of the sample after freezing, the size of the wrinkle formed in the lower part decreases with the increase of the steel fiber content, indicating that the volume of the ice lens formed during the freezing process decreased, thereby reducing the frost heave deformation accordingly.

It can be seen from Figure 8 that the moisture content at the top of the sample has increased compared with the initial value, indicating that with the generation of the temperature gradient, moisture migration will occur at the beginning of freezing. The moisture content of the position at a height of 35 mm is lower than that of the top, showing that the freezing front advances faster at this position, the time required to form frozen soil is very short, and the water migrating to the top of the sample cannot be replenished from the bottom in time. Referring to Figure 6, it can be seen that the amount of external water supply is small at this stage, and the water migration mainly occurs inside the sample. As the development speed of the freezing front in the lower part of the sample decreases, the amount of water replenishment increases, especially around the height of 15 mm. Due to the slow freezing speed and the long time for water migration, a large amount of migrated water forms ice lenses, resulting in a significant increase in the water content in this region and forming wrinkles in the lower part of the sample in Figure 7. In the lower end area of the sample, the soil moisture content at a height of 5 mm is lower than the initial value, because the moisture content decreases after the water migrates to the upper part.

By analyzing the moisture content curves under different steel fiber content conditions, it can be found that the steel fiber content has little effect on the moisture migration at the top of the sample, while for the lower part of the sample, the moisture content increases significantly. When the water accumulates to form the ice lens, the added steel fiber improves the tensile strength of the frozen soil and limits the volume growth of these ice lenses, so the water content decreases to a certain extent. At the same time, with the increase in the amount of steel fiber added, the effect of inhibiting the development of ice lenses will be improved, and the amount of water migration will be reduced accordingly, resulting in a further decrease in the water content in the sample.

4. Discussions

4.1. Influence of Steel Fibers on Temperature Distribution. When the steel fiber size is a fixed value ($l = 8$ mm, $d = 0.12$ mm), the change in the temperature distribution of the silt sample with time under the condition of different steel fiber contents is shown in Figure 9.

During the test, due to the constant temperature effect of the cold end and the warm end, the temperature at the top and bottom of the sample was always kept at -10°C and 2°C. It can be seen from Figure 9 that the temperature begins to cool from the top, and the temperature at the height of 40 mm drops to 0°C when it is frozen for 15 minutes, indicating that the freezing front advances to this position. There is a large temperature gradient within 10 mm of the top area, while the rest of the sample is in a positive temperature state with a small temperature gradient. As the freezing front advances downward, the temperature gradient in the upper 20 mm range of the sample increases significantly after freezing for 60 min, and a large temperature gradient appears in the negative temperature range of the sample. The reason is that the freezing front advances to the height of 30 mm when freezing for 30 min, and when the soil temperature drops to 0°C, the latent heat released by the freezing of water reduces the temperature gradient in the soil. Until the temperature at the 30 mm position is lower than -1°C after 60 min, a large temperature gradient will not appear in the upper 20 mm range of the sample. After freezing for 90 min, the freezing front was advanced to the height of 10 mm, and the decrease of the upper temperature made the internal temperature gradient of the sample more consistent; especially after 120 min, the temperature gradient in the whole sample height range was basically the same. Affected by the warm end, the temperature change within 10 mm of the bottom is relatively small, and it is in a positive temperature state, which ensures the condition of continuous water replenishment. As the temperature gradient within the sample is a key factor affecting the moisture migration, a large temperature gradient has not appeared at the bottom until 90 minutes of freezing; then, it caused the replenishment of external water supplement, as shown in Figure 6.

From the distribution characteristics of the temperature gradient at different times, the cooling rate is slow before dropping to 0°C, and the temperature gradient in the unfrozen area is small. The temperature distributions in the samples before and after the incorporation of steel fibers are basically the same, and with the decrease of the temperature, the temperature difference is further reduced. The temperature distribution in the sample without steel

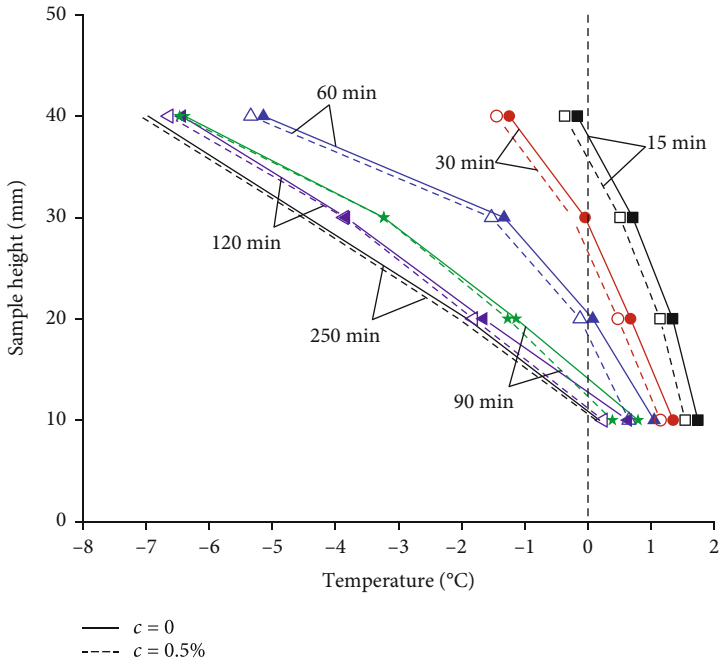

Figure 9: Temperature distribution of samples with different contents of steel fiber.

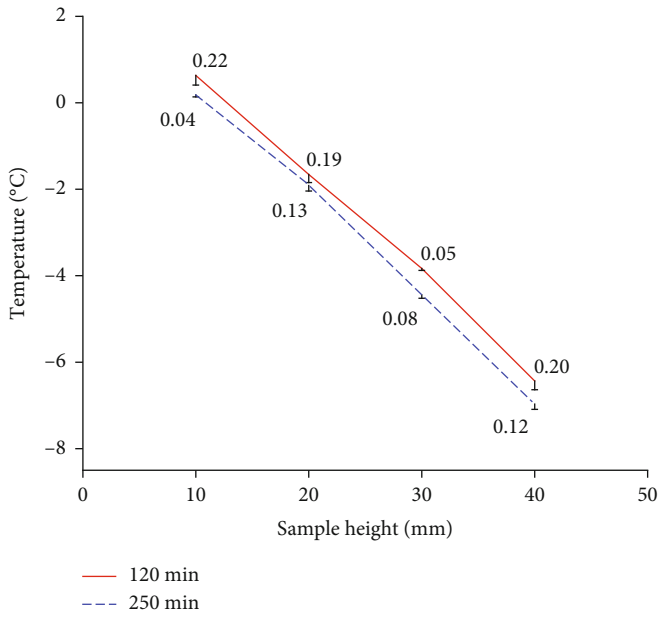

Figure 10: Temperature distribution after freezing for 120 minutes and 250 minutes.

fiber at 120 min and 240 min is shown in Figure 10, and the maximum temperature difference under the condition of different steel fiber contents is as marked in the curve. It can be seen from the figure that the maximum difference under different steel fiber content conditions is only 0.22°C when it is frozen for 120 minutes, and it is reduced to 0.13°C when it is frozen for 240 minutes. Therefore, the addition of a small amount of steel fibers will not have a significant effect on the freezing temperature distribution and its gradient inside the sample. In addition, it can be found from Figure 10 that the temperature of the steel fiber incorporated sample is slightly lower than that without steel fibers. This result shows that the steel fiber will increase the thermal conductivity of the sample, which will speed up the freezing effect to a certain extent, but the difference is small. As the freezing progresses, the thermal conductivity difference between the frozen soil and the steel fiber decreases, which further reduces the temperature difference between different measuring points.

4.2. Influence of Steel Fiber Parameters on Frost Heave Rate. In order to explore the effect of different steel fiber physical

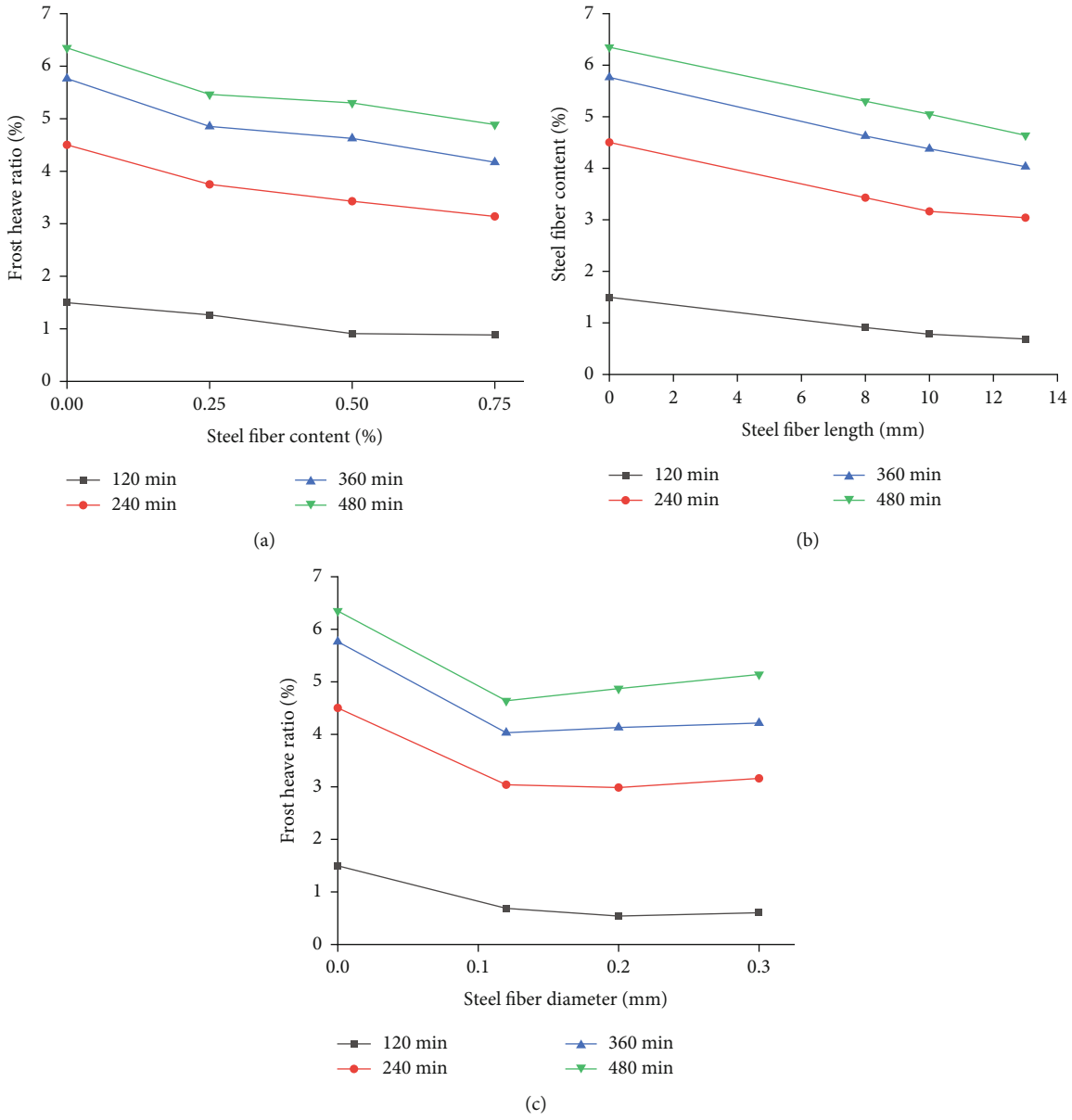

Figure 11: Variation of frost heave rate with characteristic parameters of steel fiber: (a) steel fiber content; (b) steel fiber length; (c) steel fiber diameter.

states on the frost heave of the sample, the relationship between the frost heave rate and the steel fiber content, length, and diameter was studied separately. The test results are shown in Figure 11.

For Figure 11(a), the length and diameter of steel fibers in the silt sample were controlled to be constant values, 8 mm and 0.12 mm, respectively. It can be seen that in different freezing stages, the frost heave rate decreases with the increase of the steel fiber content, and with the extension of the freezing time, the decreasing trend of the frost heave rate is more obvious. In the later stage of freezing, the segregated frost heave effect caused by the migration of moisture outside the sample dominates the total deformation, and the incorporated steel fiber can significantly improve the tensile strength of the frozen soil, thereby inhibiting the frost heave deformation. The frost heave rate decreases approximately linearly with the steel fiber content.

As shown in Figure 11(b), the frost heave rate of the sample decreases linearly with fiber length during the freezing process. At the end of freezing in the test, under the condition that the mass content of steel fiber is 5% and the diameter is 0.12 mm, the frost heave rate with steel fiber length of 8 mm, 10 mm, and 13 mm is 5.29%, 5.05%, and 4.64%. Compared with the samples without steel fibers, the reduction rate is 16.52%, 20.48%, and 26.93%, respectively. These data indicate that the reinforcement effect of the longer steel fibers is more obvious in improving the tensile strength of the frozen soil, which can more effectively improve the effect of inhibiting frost heave. Based on this result, longer steel fibers should be selected in practical

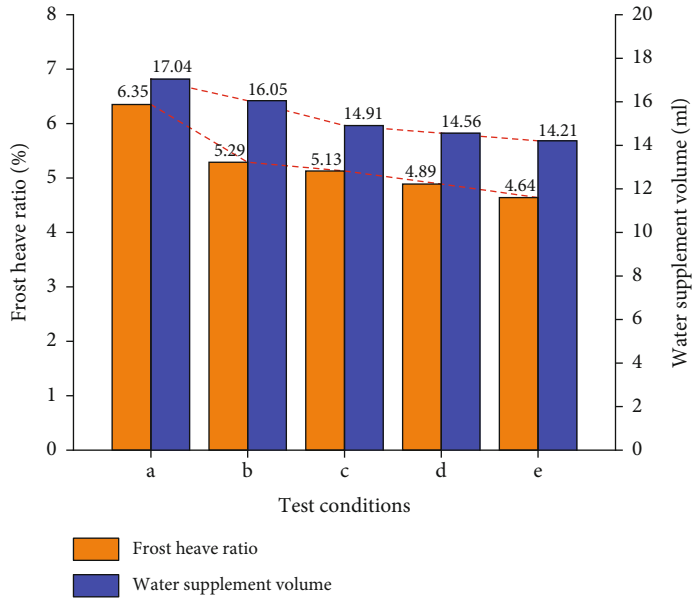

Figure 12: Variation of frost heave ratio and water supplement at different test conditions: (a) $c = 0$; (b) $c = 0.5\%$, $l = 8$ mm, $d = 0.12$ mm; (c) $c = 0.75\%$, $l = 8$ mm, $d = 0.12$ mm; (d) $c = 0.5\%$, $l = 13$ mm, $d = 0.12$ mm; (e) $c = 0.5\%$, $l = 13$ mm, $d = 0.3$ mm.

engineering, which has a better inhibitory effect on soil frost heave.

When it comes to the effect of steel fiber diameter, it can be seen from Figure 11(c) that the frost heave deformation can be suppressed by incorporating steel fibers with different diameters on the whole. Similar to the first two parameters, the significant growth stage of the frost deformation occurs during the freezing period of 120 min-240 min. The larger temperature gradient in this period leads to the rapid increase in moisture migration and the growth of the ice lens, which causes the rapid increase in deformation. Since the key to limiting the growth of ice lens is that the tensile strength of frozen soil is enhanced after the incorporation of steel fibers, under the conditions of the same amount and length parameters, as the diameter of steel fibers increases, the amount of incorporated steel fibers will be relatively reduced. This reduces the cementation between the steel fibers and the soil particles, thereby reducing the increasing trend of the soil tensile strength. Therefore, the inhibitory effect decreases with the increase of the diameter of the steel fiber. When frozen for 480 min, the frost heave rates of steel fibers with diameters of 0.12 mm, 0.2 mm, and 0.3 mm were about 4.64%, 4.89%, and 5.14%. Compared with the samples without steel fibers, the reductions were 26.93%, 23.31%, and 19.06%, respectively. When thicker steel fibers are used in construction, the amount of incorporation should be appropriately increased to improve the limiting effect of ice lens growth, thereby effectively suppressing frost heave deformation.

It is important to point out that the distribution state of steel fibers has a great influence on the frost heave deformation of the improved soil. In this paper, the effect of lap between steel fibers can actually be reacted by different length parameters, and the frost swelling difference was studied by incorporating three different lengths of steel fibers. In the distribution pattern of steel fibers, in addition to the different contents, we try to ensure the homogeneous mixing of soil particles and steel fibers during the specimen making process as much as possible to achieve a standardized sample making process. As far as the cementation state between steel fibers and soil particles is concerned, it belongs to a more microscopic research area, which is not capable to be considered in this paper at present and is subject to further study.

4.3. The Relationship between Frost Heave and Water Supplement. The cumulative water supplement and frost heave rate changes during the test are shown in Figure 12. It can be seen that at the end of the test, the frost heave rate and the accumulated water supplement amount will decrease with the steel fiber content and will also be affected by characteristic parameters such as the length and diameter. The change in the steel fiber content has a more significant effect on the frost heave rate and the accumulated water supplement. From the test results under different parameter conditions, the frost heave rate and the accumulative water supplement have the same increasing trend; the change rules of these two indicators are basically the same.

According to this phenomenon, it can be concluded that water migration from the outside of the sample is the main cause of frost heave deformation, and blocking or reducing the external water supply is the key to controlling frost heave. During the test, the dimensional changes such as the length and diameter of the steel fiber affected the freezing process by changing the external moisture migration, which was the key mechanism for the steel fiber modified soil to inhibit frost heave.

4.4. Different Soil Properties. In this experiment, frost heave was also studied through two different soil properties, silty

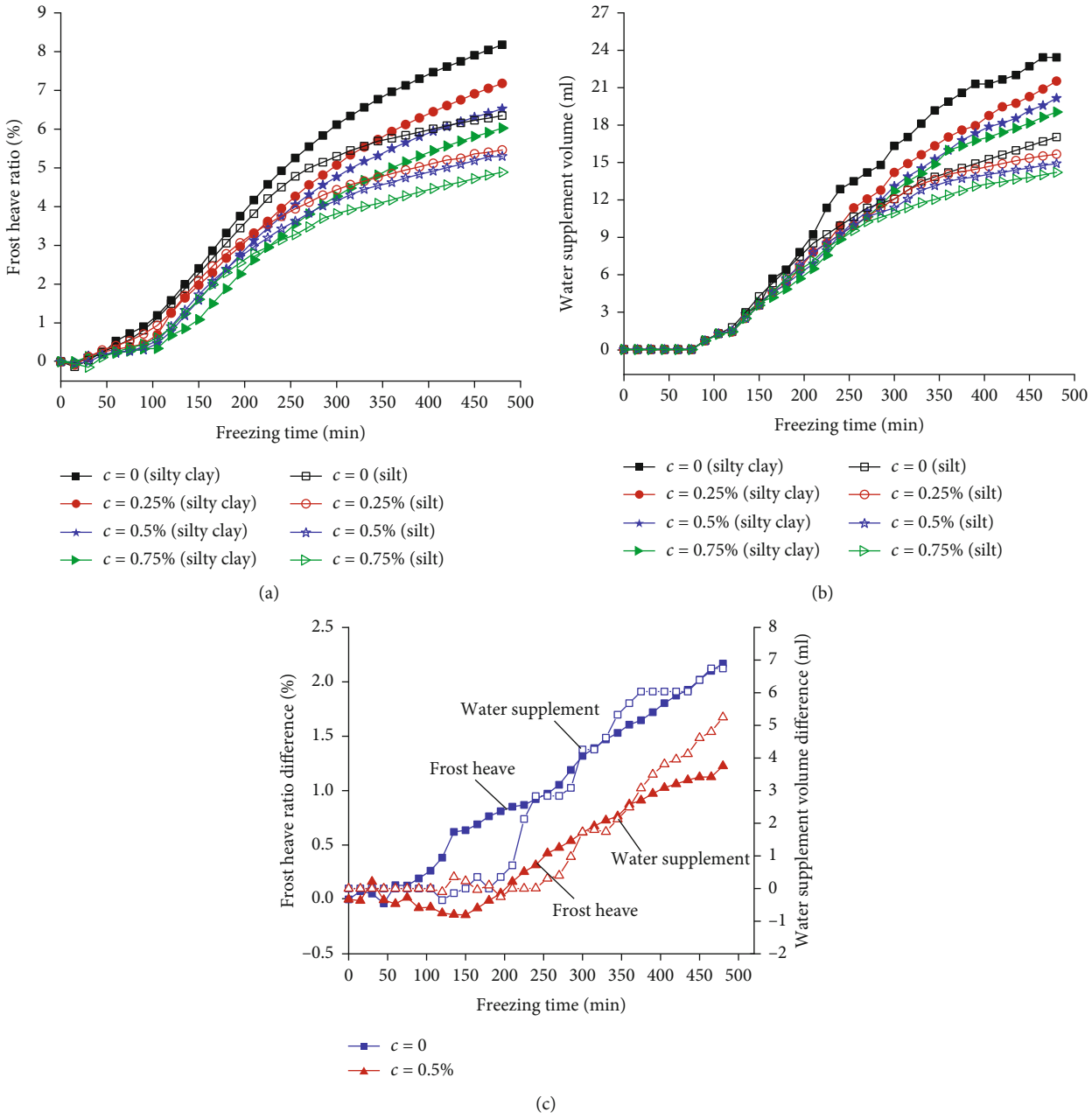

Figure 13: Comparative curves between two kinds of soil: (a) frost heave ratio; (b) water supplement; (c) difference in frost heave ratio and water supplement.

clay and silt. The frost heave ratio, water supplement, and the difference curves of these two soils are shown in Figure 13. It can be seen from Figures 13(a) and 13(b) that the development process of frost heave and water supplement curves of the two soil types are generally consistent. At the same time, it can be found that in the rapid growth stage of the moisture migration during the freezing period of 120-250 minutes, the water supplement amount is roughly the same under the conditions of different steel fiber contents, but the frost heave rate is quite different, especially in the silty clay. The reason is that the water conductivity of the fine-grained soil enhanced by the steel fiber is more obvious, and the contact area between the small-sized soil particles and the steel fiber is larger, which can significantly increase the tensile strength of the frozen soil, reduce the internal deformation, and improve the inhibition effect of frost heave deformation. Although the larger specific surface area brought by the smaller soil particle size will increase the amount of water migration and cause larger frost heave deformation, the improvement of water conductivity after the incorporation of steel fibers is correspondingly more significant. The test data show that when 0.25%, 0.5%, and 0.75% steel fibers are added to the silty clay, the water migration decreases by 8.11%, 14.09%, and 18.69% at the end of freezing, and the frost heave rate decreases by 12.24%, 20.05%, and 26.28%. In contrast, the water migration of

Table 3: Frost heave inhibition rates for two kinds of soil.

Steel fiber content	Silty clay	Silt
0.25%	12.24	10.02
0.5%	20.05	16.54
0.75%	26.28	22.99

the silt samples decreased by 8.04, 12.05, and 16.67%, and the frost heave rate decreased by 10.02%, 16.54%, and 22.99%, respectively. For more visualization, the frost heave inhibition rates for the two soil properties at different steel fiber contents are also shown in Table 3.

In order to further analyze the influence of soil properties, the difference between the frost heave ratio and the water supplement in two kinds of soil before and after incorporating steel fibers is shown in Figure 13(c). It can be seen that in the early stage of freezing, in the absence of external water supplementation, the frost heave rate of the two soils is almost the same, and the slight difference is caused by the different saturated moisture content of the soil. After 90 min of freezing, the external moisture began to migrate in, the resulting segregation frost heaving made the deformation enter a stage of rapid growth, and the difference in the frost heave rate between the two samples also began to increase. In the initial stage, the water migration caused by the smaller temperature gradient is small, and the water replenishment amount of the two samples is basically the same. After 200 min of freezing, with the obvious increase of external water recharge, the silty clay sample with smaller particle size replenished water faster, resulting in a corresponding increase in the difference between the cumulative water supplement and frost heave rate between the two samples. Since the particle size of soil particles is a critical factor affecting the water migration process, the water migration of silty clay with smaller particle size has always been greater than that of silt samples during the test, and the difference between the frost heave ratios of the two has also increased accordingly.

For the two soil properties after adding steel fibers, the difference in the amount of water supplementation between the two samples at the initial freezing stage is small. After 250 min of freezing, the difference in the limiting effect of steel fibers on the growth process of the ice lens leads to an increase in the amount of water migration in the silty clay, which makes the external water replenishment more than that of the silty sample, and this gap continued to increase as the freeze progressed. Steel fibers will change the water conductivity and deformation process in the sample, especially fine-grained soil. Therefore, during the in situ frost heave period, the cementation between the steel fibers and the soil particles with smaller particle size is better, which will significantly reduce the frost heave rate of the silty clay, resulting in a smaller in situ frost heave than silt. With the replenishment of external water, the migration of fine-grained soil is faster, and the frost heave rate of the silty clay mixed with steel fibers is always higher than that of the silt samples.

Comparing the change process of frost heave rate and accumulative water supplement of the two soils before and after adding steel fiber, steel fiber can not only reduce the difference in water migration between the two soil samples but also delay the time when the difference occurs by about 50 minutes. This is because the incorporation of steel fibers makes the lens formation time in the sample elapsed by 50 min, and the inhibitory effect of the steel fibers on the growth of the ice volume also reduces the difference in the amount of moisture migration, thereby reducing the corresponding difference of the frost heave rate. Since water migration is the main reason for the frost heave deformation of the samples, the change trend of the difference between the water supplement amount and the frost heave rate during the freezing process is consistent. However, there is a deviation in the change process after the incorporation of steel fibers; the reason is that the incorporated steel fibers also affect the deformation inside the sample. Therefore, the incorporation of steel fibers in the soil will not only limit the generation of ice lens and inhibit its volume growth but also affect the deformation process, which are the reasons for the inhibition of frost deformation in the steel fiber improved ground.

5. Conclusions

In this paper, through the one-dimensional frost heave test of steel fiber improved soil in an open system, the influence of factors such as steel fiber content, size, and soil properties on the frost heave characteristics was analyzed, and the following conclusions were obtained:

(1) The addition of a small amount of steel fibers does not have a significant effect on the freezing process and the internal temperature distribution characteristics. After 90 min of freezing, the large temperature gradient at the bottom of the sample causes the external moisture to migrate, resulting in the rapid growth of frost heave deformation

(2) The segregated frost heave caused by the migration of external moisture is the main source of frost heave deformation, and the steel fiber can improve the tensile strength of the frozen soil, inhibit the growth of the ice lens, and reduce the amount of water migration, thereby reducing the frost heave. The frost heave rate decreased by 26.93% when 0.5% steel fiber was incorporated

(3) The inhibitory effect of steel fibers increased nearly linearly with the increase of the content and length and decreased with the increase of the diameter. When the amount of steel fibers added to the silt samples was increased from 0.25% to 0.75% or the length of steel fibers was increased from 8 mm to 13 mm, the effect of inhibiting frost heave could be increased by 10.44% and 12.45%, respectively. In contrast, when the diameter of steel fibers was expanded from 0.12 mm to 0.3 mm, the frost heave inhibition effect decreased by 10.77%

(4) Steel fibers have a more significant inhibitory effect on water migration and frost heave in fine-grained

soil. When the content of steel fiber is 0.75%, the frost heave rate of silty clay is 14.31% lower than that of silt, and the water migration is 11.99% lower

Data Availability

Some or all data, models, or codes that support the findings of this study are available from the corresponding author upon reasonable request.

Conflicts of Interest

The authors declare that they have no conflicts of interest.

Acknowledgments

This research was supported by the National Natural Science Foundation of China (No. 52108386) and the National High-tech Research and Development Program (863 Program) (No. 2012AA06A401). The authors are deeply indebted to these financial supporters.

References

[1] Y. Wang, Z. Y. Song, T. Q. Mao, and C. Zhu, "Macro-meso fracture and instability behaviors of hollow-cylinder granite containing fissures subjected to freeze–thaw–fatigue loads," *Rock Mechanics and Rock Engineering*, vol. 55, no. 7, pp. 4051–4071, 2022.

[2] Y. Wang, J. Q. Han, Y. J. Xia, and D. Long, "New insights into the fracture evolution and instability warning predication for fissure-contained hollow-cylinder granite with different hole diameter under multi-stage cyclic loads," *Theoretical and Applied Fracture Mechanics*, vol. 119, article 103363, 2022.

[3] Y. Y. Zhou, J. J. Zhang, and S. J. Yan, "Advance and review on the experimental researches of the freezing and thawing characteristics of soils," *Chinese Journal of Rock Mechanics and Engineering*, vol. 41, no. 6, pp. 1267–1284, 2021.

[4] W. She, X. Y. Cao, G. T. Zhao, D. Cai, J. Jiang, and X. Hu, "Experimental and numerical investigation of the effect of soil type and fineness on soil frost heave behavior," *Cold Regions Science and Technology*, vol. 148, pp. 148–158, 2018.

[5] T. L. Wang and Z. R. Yue, "Influence of fines content on frost heaving properties of coarse grained soil," *Rock and Soil Mechanics*, vol. 34, no. 2, pp. 359–365, 2013.

[6] J. Z. Zhou, C. F. Wei, and D. Q. Li, "Experimental study and numerical simulation to the process of frost heave in saturated silt," *Chinese Journal of Rock Mechanics and Engineering.*, vol. 36, no. 2, pp. 485–495, 2017.

[7] F. Y. Liu, Z. S. Shao, R. J. Qiao, S. Zhang, and W. C. Cheng, "The influence of compaction energy on frost-heave characteristics of coarse-grained soil," *Natural Hazards.*, vol. 100, no. 2, pp. 897–908, 2020.

[8] J. H. Chen, "Study on the frost heave characteristics of artificial frozen soil under different freezing mode," *Progress in Industrial and Civil Engineering.*, vol. 204-208, pp. 599–603, 2012.

[9] K. Hu, G. Q. Zhou, and X. J. Li, "Experiments on frost heave of artificial frozen soils with different constraints," *Journal of China Coal Society.*, vol. 36, no. 10, pp. 1653–1658, 2011.

[10] Y. P. Shen, T. X. Tang, R. F. Zuo, Y. Tian, Z. Zhang, and Y. Wang, "The effect and parameter analysis of stress release holes on decreasing frost heaves in seasonal frost areas," *Cold Regions Science and Technology.*, vol. 169, p. 102898, 2020.

[11] J. S. Zhou, G. Q. Zhou, and W. Ma, "Experimental research on controlling frost heave of artificial frozen soil with intermission freezing method," *Journal of China University of Mining & Technology.*, vol. 35, no. 6, pp. 708–712, 2006.

[12] G. Q. Zhou, K. Hu, X. Y. Shang, and J. S. Zhou, "Test and numerical simulation on frost heave in frozen soils in intermittent freezing mode," *Proceedings of the International Conference on Mining Science & Technology.*, vol. 1, no. 1, pp. 512–518, 2009.

[13] Y. Zhou and G. Q. Zhou, "Intermittent freezing mode to reduce frost heave in freezing soils - experiments and mechanism analysis," *Canadian Geotechnical Journal.*, vol. 49, no. 6, pp. 686–693, 2012.

[14] L. Huang, Y. Sheng, and X. B. Huang, "Experimental study on force and deformation of soil during unidirectional frost heaving under different paths. Chinese," *Journal of Geotechnical Engineering*, vol. 38, no. Suppement.2, 2019.

[15] C. P. Han, D. P. He, and Y. M. Jia, "Frost heave properties of lime modified subgrade soil," *Journal of Chang'an University (Natural Science Edition).*, vol. 33, no. 3, pp. 27–31, 2013.

[16] L. H. Tan, *Investigation on Properties of Frost Heave and Thawing Settlement of Cement-Improved Soil the Degree of Master*, Tongji University, Shanghai, 2006.

[17] X. D. Hu, "Laboratory research on properties of frost heave and thaw settlement of cement-improved Shanghai's grey-yellow silty sand," *Journal of China Coal Society.*, vol. 34, no. 3, pp. 334–339, 2009.

[18] Y. M. Song, *Study on Properties of Frost Heave and Thawing Settlement of Cement-Improved Silty Clay the Degree of Master*, China University of Mining & Technology, Xuzhou, 2018.

[19] Z. Li, S. H. Liu, L. J. Wang, and C. Zhang, "Experimental study on the effect of frost heave prevention using soilbags," *Cold Regions Science and Technology.*, vol. 85, pp. 109–116, 2013.

[20] K. Hu, X. Q. Chen, J. G. Chen, and X. Ren, "Laboratory investigation of the effect of nano-silica on unconfined compressive strength and frost heaving characteristics of silty clay," *Soil Mechanics and Foundation Engineering.*, vol. 55, no. 5, pp. 352–357, 2018.

[21] L. Chen, R. P. Guo, and G. X. Li, "Research on preventing soil frost heave with geotechnical reinforcement," *Journal of Hydraulic Engineering*, vol. 3, pp. 84–88, 1996.

[22] X. Q. Liu, J. K. Liu, Y. H. Tian, Y. Shen, and J. Liu, "A frost heaving mitigation method with the rubber-asphalt-fiber mixture cylinder," *Cold Regions Science and Technology.*, vol. 169, pp. 102912–102918, 2020.

[23] A. A. S. Correia and P. J. V. Oliveira, "Strength of a stabilised soil reinforced with steel fibres," *Proceedings of the Institution of Civil Engineers-Geotechnical Engineering*, vol. 170, no. 4, pp. 312–321, 2017.

[24] Y. Wang, T. Mao, Y. Xia, X. Li, and X. Yi, "Macro-meso fatigue failure of bimrocks with various block content subjected to multistage fatigue triaxial loads," *International Journal of Fatigue*, vol. 163, p. 107014, 2022.

[25] R. J. Shi, F. Huang, and F. T. Yue, *A Method for Suppressing Frost Heave Deformation of Fiber-Improved Ground*, no. 5, 2021China, 2021.

[26] Y. Wang, Y. Su, Y. Xia, H. Wang, and X. Yi, "On the effect of confining pressure on fatigue failure of block-in-matrix soils exposed to multistage cyclic triaxial loads," *Fatigue & Fracture*

of Engineering Materials & Structures., vol. 45, no. 9, pp. 2481–2498, 2022.

[27] J. M. Konrad and N. R. Morgenstern, "The segregation potential of a freezing soil," *Canadian Geotechnical Journal*, vol. 18, no. 4, pp. 482–491, 1981.

[28] J. Zhou, C. Wei, H. Wei, and L. Tan, "Experimental and theoretical characterization of frost heave and ice lenses," *Cold Regions Science and Technology*, vol. 104-105, no. 3, pp. 76–87, 2014.